Defense Technical Information Center Compilation Part Notice

ADP011118

TITLE: Yaw Control at High Angles of Attack Through Vortex Manipulation Using Rotating Nose Strakes

DISTRIBUTION: Approved for public release, distribution unlimited

This paper is part of the following report:

TITLE: Active Control Technology for Enhanced Performance Operational Capabilities of Military Aircraft, Land Vehicles and Sea Vehicles [Technologies des systemes a commandes actives pour l'amelioration des performances operationnelles des aeronefs militaires, des vehicules terrestres et des vehicules maritimes]

To order the complete compilation report, use: ADA395700

The following component part numbers comprise the compilation report:
ADP011101 thru ADP011178

Yaw Control at High Angles of Attack Through Vortex Manipulation Using Rotating Nose Strakes

Peter R. Hakenesch
DaimlerChrysler Aerospace - Military Aircraft
P.O. Box 801160, 81663 München, Germany
peter.hakenesch@m.dasa.de

Abstract
The effect of nose strakes on the flow field in the vicinity of the forward fuselage section of an aircraft was investigated. Emphasis was placed on the manipulation of the vortices in order to generate a significant side force and yawing moment with the purpose not only to stabilize the aircraft at high angles of incidence, but also to achieve yaw control. Aside from conventional control surfaces, an additional control device was realized by mounting a single strake on the nose section which could be rotated around its longitudinal axis. Experimental force and pressure data from low speed wind tunnel tests indicate the potential of this control device for aircraft flying at high angles of attack.

List of symbols

b	[m]	Wing span
C_l	[-]	Rolling moment coefficient
C_m	[-]	Pitching moment coefficient
C_n	[-]	Yawing moment coefficient
C_{lp}	[rad^{-1}]	Roll damping derivative
l_{ref}	[m]	Reference length
M_∞	[-]	Mach -number
p, q, r	[rad/s]	Rotation rates around x_f, y_f, z_f
S_{ref}	[m^2]	Reference area
v	[m/s]	Velocity
α	[deg]	Angle of attack
β	[deg]	Sideslip angle
η	[deg]	Flap deflection
Λ	[-]	Aspect ratio b^2/S_{ref}
φ	[deg]	Radial Strake position
x, y, z	[m]	Coordinates

Subscripts

a	Aerodynamic axis system
b	Body axis system
ref	Reference
∞	Free stream conditions

Abbreviations

BAR	Bihrle Applied Research
C	Canard
HARV	High Angle of Attack research Vehicle
LAMP	Large Amplitude Test Facility
LEF	Leading Edge Flap
MAC	Mean Aerodynamic Chord
MATV	Multi Axis Thrust Vectoring
R	Rudder
TEF	Trailing Edge Flap
W	Winglet

1. Introduction

Aircraft maneuvering at high angles of attack are faced with a dramatic loss of control power in yaw as the rudder almost loses completely its efficiency beyond 40 degrees angle of attack. So far, the only possibility to conduct controlled flights at angles of attack reaching into the post stall regime, is to take advantage of thrust vectoring, as demonstrated successfully by the experimental aircraft F-18 HARV, X-31 or F-16 MATV, Fig. 1. All three aircraft are flown in different programs and were developed independently. The NASA F-18 HARV is a testbed to produce aerodynamic data at high angles of attack to validate computer codes and wind tunnel research. The X-31 is being used to study thrust vectoring to enhance close-in air combat maneuvering, while the F-16 MATV is demonstrating how thrust vectoring can be applied to operational aircraft. Another promising possibility, aside from thrust vectoring, to control an aircraft in this angle of attack region, is to actively manipulate the vortices developing at the nose and fuselage through pneumatic devices such as different forms and directions of blowing or suction, or through mechanical devices such as strakes.

Fig. 1: Thrust vectoring aircraft

Paper presented at the RTO AVT Symposium on "Active Control Technology for Enhanced Performance Operational Capabilities of Military Aircraft, Land Vehicles and Sea Vehicles", held in Braunschweig, Germany, 8-11 May 2000, and published in RTO MP-051.

This paper deals with the possibilities to achieve vortex control and subsequently yaw control by introducing a controlled disturbance into the flow in the nose tip region of the aircraft through the use of a movable micro-strake.

The general structure of the vortex system around a slender body or an aircraft fuselage is indicated in Fig. 2. At low and moderate angles of attack (α_1), the flow still follows the contour and no vortices are formed. The resulting normal force increases linearly with angle of attack and no side force is generated. At more elevated angles of attack (α_2), the flow starts to separate from the fuselage and symmetric vortices are created. This leads to a non-linear increase of the normal force, similar to the non-linear lift curve of a delta wing. Due to the symmetric and basically stable vortex structure, side forces are virtually nonexistent. At even higher angles of attack (α_3), a quasi-stable but asymmetric vortex structure forms, which causes a considerable side force as well as a strong normal force. The side force may reach the same magnitude as the normal force but will again decrease and finally disappear again, as the angle of attack is further increased.

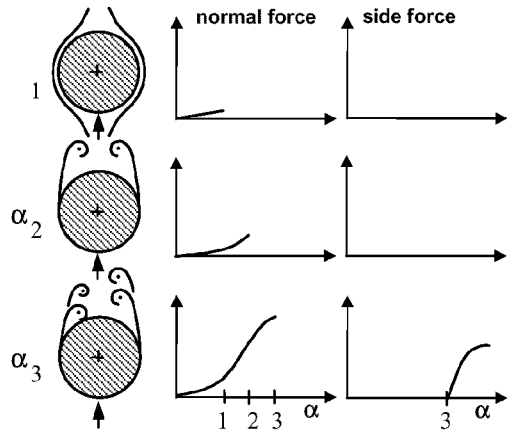

Fig. 2: Vortex structures and normal- and side forces vs. angle of attack [5]

Significant research concerning the use of forebody strakes for vortex control has been carried out so far. Two major fields of application can be distinguished: One consists of a pair of strakes positioned symmetrically in the nose region of the aircraft fuselage with the main purpose of forming and stabilizing a symmetric vortex structure in order to avoid the generation of asymmetric side forces or the switching from one quasi-stable state to another. The second group of application is not so much focussed on stabilizing but on actually controlling the aircraft. Control input is realized by two strakes which are located symmetrically in the nose area at fixed positions, and can be deployed and retracted. This concept was successfully flight tested in the F-18 HARV, Fig. 3. In order to use the nose strake as an operational control device with an efficiency similar to a conventional rudder, a control function must be established that describes the achievable forces and moments as a function of the flow conditions, aircraft attitude and strake position. The application under investigation in this study allows the positioning of the strake at any radial position on the nose depending on the control forces required for a specific maneuver.

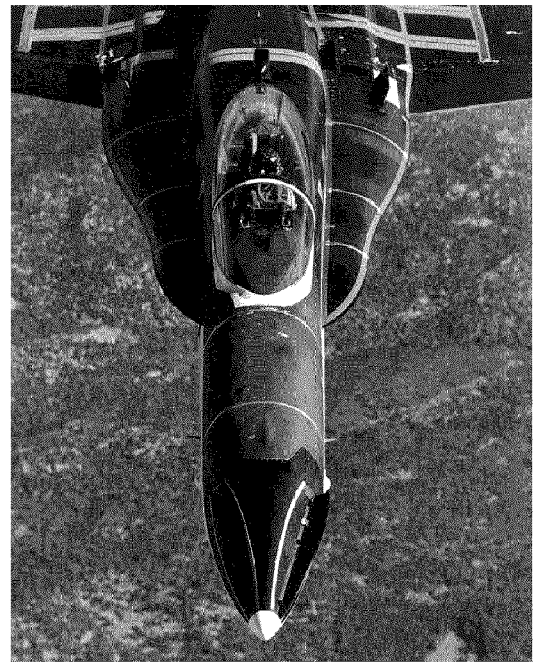

Fig. 3: F-18 HARV Nose strake deployed

2. Experimental setup

Due to an extensive, and also flight test validated data base, all tests were carried out with a 1:7.5 scale model of the X-31 in the low speed wind tunnel LAMP of BAR Neuburg, Germany, Fig. 4. This test facility allows for static as well as dynamic testing in the low speed regime. Maximum free stream velocity in the 10ft vertical test section is 40 ft/s. The range of angle of attack is ±180° and the sideslip range is ±32°. For evaluation of dynamic characteristics, the model can be rotated around the wind-vector axis up to 150 rpm. A forced oscillation with maximum amplitudes of up to 40° around any of the body axis can be superimposed to the rotational movement.

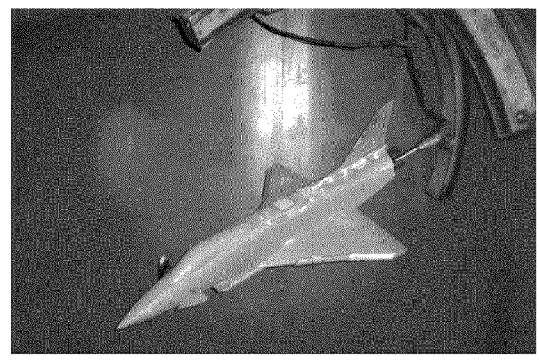

Fig. 4: X-31 Force model in LAMP test section

The nominal test conditions as well as the model reference data are listed in Tab. 1.

Tab. 1: X-31 Reference data

Scale			1:7.5
Reference area	S_{ref}	[m²]	0.3738
Reference length	l_{ref} = MAC	[m]	0.502
Reference point	$c.g._{ref}$	[m]	0.908
Wing span	b	[m]	0.968
Free stream velocity	v_∞	[m/s]	10.83

As the size of the strake is of lesser importance than its position, a parametric study to specify the minimum strake size still suitable to have a noticeable effect on the vortex structure, was carried out, Fig. 5. As shown in the results, Fig. 7, even the smallest strake tested (no.1: 1/2"x1/8") and selected for subsequent determination of its efficiency function, showed little deviation from the larger sizes with respect to its effect on the achievable yawing moment and side force.

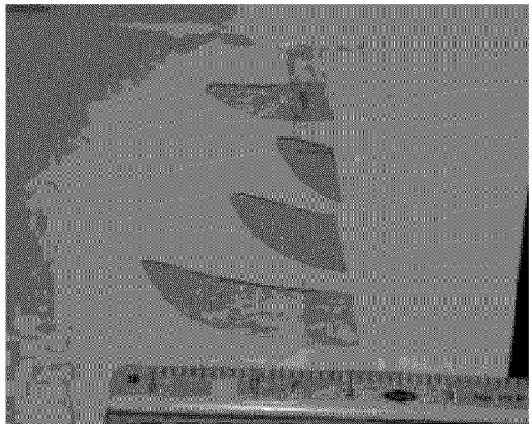

Fig. 5: Strakes tested, 2"x1/2" through 1/2"x1/2"

In order to determine the induced forces and moments as a function of angle of attack, sideslip and radial position of the strake, a modified nose section was designed for the X-31 force model which allowed the movement of the strake to any desired radial position by rotating the nose around its longitudinal axis, Fig. 6.

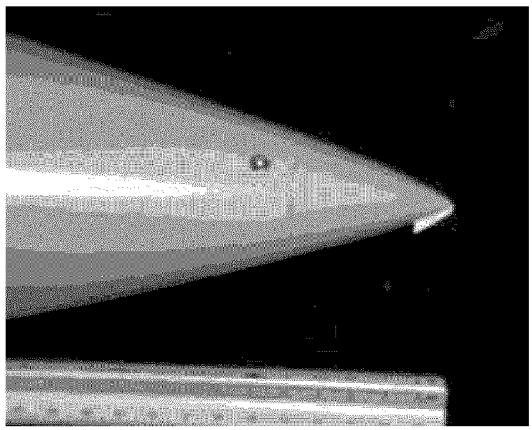

Fig. 6: Modified nose section - rotating around its longitudinal axis with strake

3. Results

During the investigation of strake position and strake efficiency, it became obvious that the actual size of the strake was of minor importance. The flow field around the forebody section seems to be fairly unstable and the vortex system formed at higher angles of attack tends to acquire one of the two possible quasi-stable and asymmetric states. The resulting flow turning direction can be influenced by even microscopic disturbances in the very beginning of the flow onset at the forebody. Therefore the size of the strakes plays a lesser role, as long as they are located at the tip of the nose. The yawing moments achievable by strakes of different sizes are shown in Fig. 7 for a strake positioned at the nose tip and rotated to a radial position of $\varphi = -30°$. Even though the efficiency of the strakes seems to depend stronger from the aspect ratio Λ than from the strake size, the results shown in Fig. 7 do not allow to establish an explicit function that relates strake efficiency, aspect ratio and strake size. The fact, that the strakes no.1 and no.2, with aspect ratios of $\Lambda = 4$ and 8 respectively, which are the smallest in size, show the maximum efficiency at an angle of attack of $\alpha = 50°$, even above strakes of larger size, confirm the general trend that size is of lesser importance than aspect ratio.

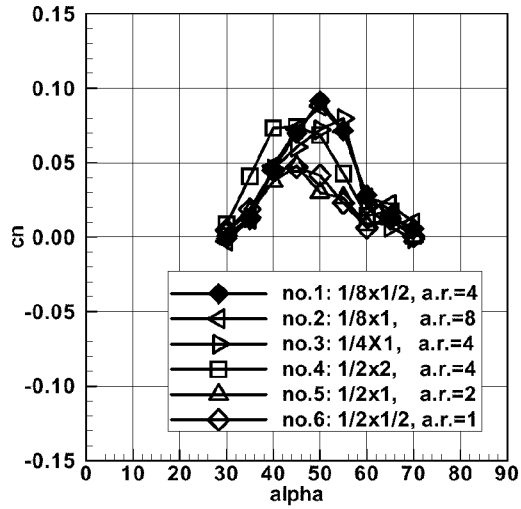

Fig. 7: Yawing moment as function of strake size

The pressure field induced at the foreward fuselage section by positioning one strake at an asymmetric position, i.e. $\varphi = -45°$, is shown in Fig. 8 for an angle of attack of $\alpha = 50°$. The strong vortex on the right hand side induces a suction force on the foreward fuselage, which due to the large distance from the center of gravity, creates the considerable yawing moments.

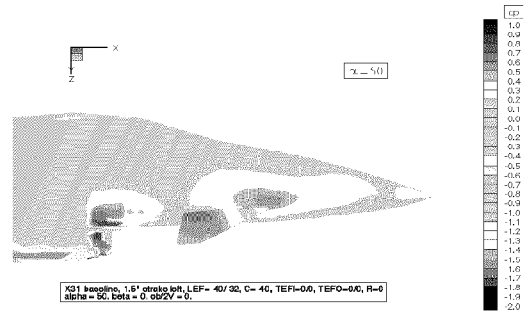

Fig. 8: Pressure distribution on nose section

The control power as a function of angle of attack and sideslip angle is shown in Fig. 9. The strake (no.1: 1/8"x1/2") is positioned at a radial position of $\varphi = -45°$. It becomes obvious, that full control power is available at angles of attack above $\alpha = 30°$ and can be maintained at positive and negative sideslip angles. For the sake of comparison, the rudder efficiency of the X-31 rudder, deflected to the maximum angle of $\eta = 30°$, is also depicted. Two aspects should be considered: First, the nose strakes allow yaw control of the aircraft at angles of attack where the conventional rudder has already lost its efficiency for good. So far, yaw control in this regime, i.e. $35° < \alpha < 70°$ was reserved to aircraft featuring thrust vector control, but could now be expanded to more conventional aircraft as well by incorporating a rotating nose strake in the fuselage nose section. Second, this tremendous control power is achieved with micro-strakes, with a full scale size of only 0.002 m² (= 3.5 square inch). As shown in Fig. 7, the actual size of the strake is of minor importance, therefore a further miniaturization seems possible. This should be considered, as any disturbances of the radar integrated in the radom are to be avoided or at least they should be minimized.

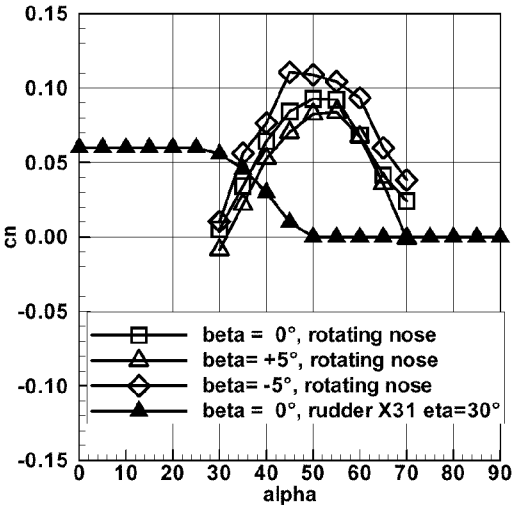

Fig. 9: Yawing moment vs. angle of attack

In order to use the rotating nose strake as a control surface, analogous to a rudder, a unique function must be established, that relates the achievable yawing moment C_n to the flow conditions α, β, M_∞, aircraft attitude and radial position φ of the nose strake. Fig. 10 shows the dependency of the yawing moment from the radial strake position φ for an angle of attack of α=45° and sideslip angles of $\beta = 0°, \pm 5°$. The experiments indicated that for large parts of the flight envelope, a linear dependency between radial strake position and yawing moment was established and therefore the usefulness of the rotating nose as a control device could be underlined.

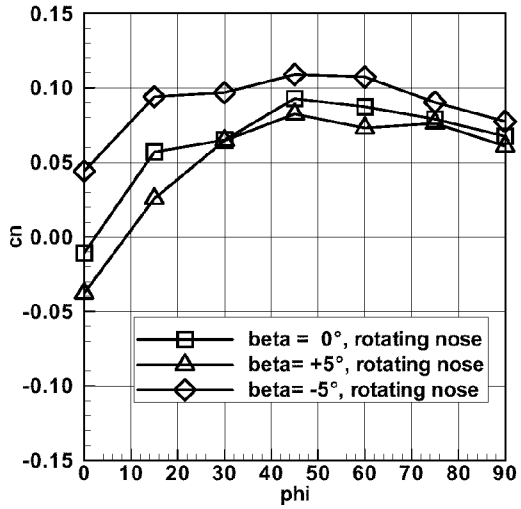

Fig. 10: Yawing moment vs. radial strake position

Another aspect to be considered are the coupled moments induced by the nose strake, i.e. the rolling moment C_l and the pitching moment C_m. As expected, the induced rolling moment due to an activated nose strake can more or less be neglected, Fig. 11. Even though the forces acting on the foreward fuselage section to generate a rolling moment are in the same order of magnitude as those responsible for the generation of the yawing moment, the resulting moment around the longitudinal axis is small, due to the very short hinge arm.

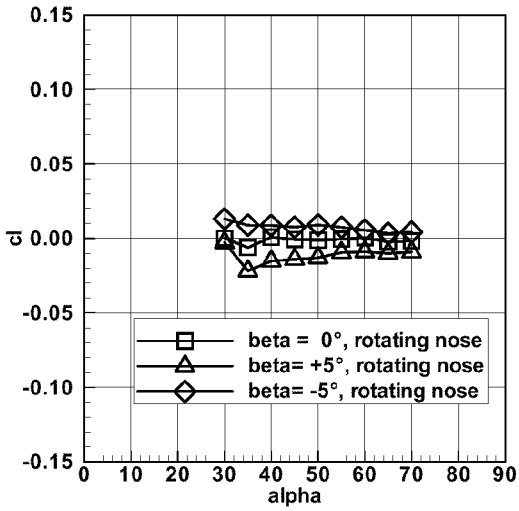

Fig. 11: Induced rolling moment due to a strake

The pitching moment due to an activated nose strake are considerably higher than the induced rolling moments Fig. 12, but are still within the margin that can be controlled by the elevator.

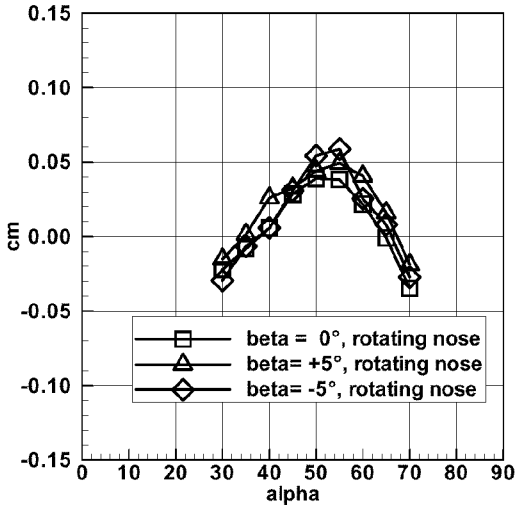

Fig. 12: Induced pitching moment due to a strake

Another possible application of nose strakes, besides yaw control in the high alpha range, is the potential for spin recovery, especially the recovery from a flat spin. Aerodynamic control devices like the rudder are of little use due to separated flow and in most cases a chute is required for spin recovery. However, the forward section of the fuselage encounters a very high relative flow angle at which the nose strakes can be used to produce adverse yawing moments to slow down and stop the rotating movement of the aircraft. As shown in Tab. 2, the yawing moment produced by the strake should be sufficient to recover an X-31-like aircraft.

Tab. 2: X-31 Mass and Inertia Data

Wing surface S	21.024	m^2
Wing half span $b/2$	3.480	m
Mass m	6067.807	kg
Inertia moment x-axis I_{xx}	4465.346	kg· m^2
Inertia moment y-axis I_{yy}	48137.355	kg· m^2
Inertia moment z-axis I_{zz}	49049.676	kg· m^2
Inertia moment fan	3.375	kg· m^2
Thrust vector angle σ	0.	deg
Altitude H	MSL	m
Spin rate ω_z	80	deg/s
Radial velocity at nose tip v_r	10.22	m/s
Sink rate v_z	75 - 100	m/s
Dynamic pressure q	3509 - 6189	Pa
Local flow angle at nose tip α_r	80 - 82	deg
Yawing moment coefficient C_N	0.3 - 0.2	-

For the maximum load condition, the yawing moment due to a deployed nose strake which is rotated to its optimum position is

$$N = C_N \cdot q \cdot S \cdot \frac{b}{2} = 90561\ Nm\ .$$

Assuming that the moments are decoupled, the damping rate around the z-axis computes to

$$\dot{\omega}_z = \frac{N}{I_{zz}} = \frac{90561}{49049} = 1.85\ rad/s^2 \approx 106\ deg/s^2\ .$$

A comparison with an assumed flat spin rate of $\omega_Z = 80$ deg/s shows, that complete spin recovery is achievable already after 0.75 s or less than one rotation around the z-axis.

4. Summary

A nose rotating around its longitudinal axis, with a fixed or deployable strake can be used as a precise steering device, similar to a rudder to achieve yaw control at angles of attack which have been previously reserved to aircraft featuring thrust vector control. During a series of static and dynamic force and pressure measurements, the optimum radial position of the strake was determined as a function of angle of attack and sideslip. The influence of the nose strake on coupled moments, i.e. rolling moment and pitching moment was measured. It became obvious that at higher angles of attack, not only the efficiency of the nose strakes was higher than that of a conventional rudder with respect to yaw control, but also for large parts of the flight envelope, a linear dependency of the achievable yawing moment as a function of the radial position of the strake was apparent. This is very remarkable, insofar as the tested micro-strakes are of very limited size, approximately 3.5 square inches or 0.002 m^2. In a subsequent step, it should be considered to integrate this concept as an additional steering device into a testbed, capable of controlled flight in the post-stall region, e.g. the X-31.

Acknowledgements

The results presented in this paper were achieved under a research contract granted by the BWB, Koblenz, Germany to DaimlerChrysler Aerospace AG, München.

References

[1] Bihrle W.: *Description of the LAMP facility Neuburg, FRG*, personal communications, 1996

[2] Ericsson L.E.: *Fluid/Motion Couplin in Conceptional Spermaneuvers*, AIAA 96-0787

[3] Klute S.M., Telionis D.P.: *The unsteady characteristics of the flow over an F/A-18 at high alpha*, AIAA 96-824

[4] Fisher D.F., Cobleigh B.R.: *Contolling Forebody Asymmetrics in Flight - Experience with Boundary Layer Transition Strips*, NASA-TM-4595, July 1994

[5] Malcolm G.N.: *Forebody Vortex Control*, AGARD-R-776-6

[6] Malcolm G.N., Ng T.T., Lewis L.C.: *Development of non-conventional control methods for high angle of attack using vortex manipulation*, AGARD-CP-465

[7] Malcolm G.N., Ng T.T.: *Aerodynamic Control of Fighter Aircraft by Manipulation of Forebody Vortices*, AGARD-CP-497-15

[8] Ng. T.T., Malcolm G.N: *Aerodynamic Control Using Forebody Strakes*, AIAA-91-0618

[9] Phillips E.H.: *F/A-18 HARV Exploits Forebody Controls*, Aviation Week & Space Technolgy, Nov. 20, 1995

Paper #21

Q by Dr. John E. Lamar: Has the author considered mounting nose strake on a nose boom? Nose strake parameters of size and aspect ratio were considered. What about strake Leading Edge shaping?

A. (Dr. P.R. Hakenesch): No, as it was intended for production in which the nose boom may not be present; also, radar across section could be a problem with a nose boom and strake. Due to limits of time and money constraints, only one shaping was considered; but it should/could be.